Estuarine, Coastal and Shelf Science 298 (2024) 108639

Contents lists available at ScienceDirect

Estuarine, Coastal and Shelf Science

journal homepage: www.elsevier.com/locate/ecss

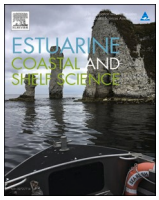

Satellite remote sensing can provide semi-automated monitoring to aid coastal decision-making

Joseph Agate [a,*], Rhoda Ballinger [b], Raymond D. Ward [c,d]

[a] Centre for Aquatic Environments, University of Brighton, Cockcroft, Moulsecoomb, Brighton, BN2 4GJ, UK
[b] School of Earth and Environment, Cardiff University, Park Place, Cardiff, CF10 3AT, UK
[c] School of Geography, Queen Mary University of London, Mile End, London, E1 4NS, UK
[d] Institute of Agriculture and Environmental Sciences, Estonia University of Life Sciences, Kreutzwaldi 5, EE-51014, Tartu, Estonia

ARTICLE INFO

Keywords:
Salt marshes
Coastal management
Coastal wetlands
Coastal monitoring

ABSTRACT

Coastlines are projected to face unprecedented pressures over the next century due to climate change-induced changes in sea level, storm, wave, and tidal regimes. This projection of increasing pressure is driving a reappraisal of existing shoreline management practices, with both science and policy calling for future strategies to work with the natural protection provided by coastal habitats such as salt marshes. However, we currently lack the understanding of long-term ecosystem dynamics required to incorporate these habitats into the definitive predictions of risk relied on in coastal protection planning. Satellite remote sensing has the potential to provide data that could address this knowledge gap with its frequent repeat times and global coverage facilitating the production of high temporal frequency time-series over large areas. This study sought to explore this potential in one of the largest coastal plain estuaries the in the UK, the Severn Estuary. The Random Forest machine learning algorithm was used to develop a time-series of marsh extents across the estuary from 1985 to 2020 in Google Earth Engine, with widths also extracted as a proxy for the marshes' protective capacity. These changes were monitored in six areas that contained the most significant areas of salt marsh across the estuary. This analysis revealed a significant increasing trend in extent and widths ($p < 0.05$), and therefore natural coastal protection, in three of the six areas over the study period, with validation testing finding an overall accuracy for the classification of >90% and a strong agreement found between the detected widths and those found in previous surveys. These findings demonstrate that satellite remote sensing combined with machine learning has the potential to provide valuable insights into changes in the extents of marshes and therefore their protective capacity. This information can be useful in the coastal planning process, allowing decision-makers to assess the sustainability of existing defences fronted by marshes, as well as allowing them to make informed decisions about the location of restoration schemes.

1. Introduction

Traditionally, coastal management has attempted to hold back the sea through built defences (French, 2004). However, climate change is projected to cause increased pressure on coastal systems through relative sea level rise (rSLR) (Nerem et al., 2018), as well as changing storm, wave and tidal regimes (Pickering et al., 2017; Reguero et al., 2019). This pressure is driving a reappraisal of management strategies, with calls for an increasing use of 'ecosystem-based' approaches which work with the natural protection provided by coastal habitats (Temmerman et al., 2013; UNEP, 2016).

A commitment to an ecosystem-based approach has been formalised in the United Kingdom (UK) within a recent government policy statement on flood and coastal erosion risk management (FCERM), which states an intention to "double the number of government-funded projects which include nature-based solutions to reduce flood and coastal erosion risk" (Defra, 2020). In England and Wales, this policy is to be implemented through Shoreline Management Plans (SMPs), which are non-statutory documents that are coordinated at a regional scale defined by discrete, littoral sediment cells that sub-divide the coast into Policy Units (PUs). Each PU is classified into one of four management strategies: No Active Intervention (NAI), Advance the Line (ATL), Hold the Line (HTL) or Managed Realignment (MR) which are assigned for policy epochs (20-, 50-, and 100-years). This strategy has been celebrated for

* Corresponding author.
E-mail address: J.E.Agate@brighton.ac.uk (J. Agate).

https://doi.org/10.1016/j.ecss.2024.108639
Received 31 March 2023; Received in revised form 18 December 2023; Accepted 12 January 2024
Available online 14 January 2024

its strategic and holistic approach to managing coastal risk, particularly in the EUROSION project (Salman and Lombardo Doody, 2004), with similar strategies developed elsewhere such as in Abu Dhabi, India, and the United States of America (Pontee, 2017; Noujas and Thomas, 2018). However, a recent review by Ballinger and Dodds (2020) found that many plans lack a scientific basis in the decision-making process, which is fundamental for effective adaptive coastal planning (Pontee, 2017).

Salt marshes are an important feature in many ecosystem-based strategies. Existing marshes reduce the requirement for built defences, and the realignment of defences and subsequent restoration of marshes have been suggested as a method to increase the protective capacity in areas where HTL policies are no longer sustainable. The interest in marshes stems from their effectiveness at protecting coastlines. This is caused largely by their high position within the tidal frame (Callaghan et al., 2010; Bouma et al., 2014) and is enhanced by surface roughness induced by often dense vegetation (Möller, 2006; Möller et al., 2014). Combined, these factors allow marshes to significantly attenuate wave energy, with estimates suggesting that 50% of wave height can be reduced over the first 10–20 m of salt marsh (Möller et al., 1999; Möller and Spencer, 2002) and that an 80 m strip reduces the height of sea wall required from 12 m to 3 m (King and Lester, 1995). This protective ability makes salt marshes extremely cost-effective, with the area of salt marshes fronting sea walls around England suggested to give capital cost savings of £13–32 billion and annual maintenance savings of £0.3 billion (Beaumont et al., 2006; Jones et al., 2011).

However, despite an appreciation for the value of marshes, there is limited understanding of long-term changes in their extents (Bouma et al., 2014). This understanding is vital in shoreline management for two reasons. Firstly, as their capacity to protect coastlines and thus reduce requirements for built structures is influenced largely by their extent (Willemsen et al., 2020), changes should be understood to provide an accurate review of coastal protection. Secondly, restoration of marshes through managed realignment has been suggested as a feasible strategy for coastal protection, with current SMPs implying an increase of 400 ha per year (Committee on Climate Change, 2018). However, the successful implementation of these schemes relies upon a sound understanding of estuarine dynamics. As a result, it is essential this knowledge gap is addressed if marshes are to be included in definitive predictions of risk relied on in coastal protection planning (Bouma et al., 2014; Brown, 2022). This understanding would also be greatly beneficial for other application such as blue carbon accounting (Luisetti et al., 2013; Macreadie et al., 2019; Bertram et al., 2021) and insuring adherence to legislative requirements for habitat protection, such as through the Conservation of Habitats and Species Regulations 2017; HM Government (2017), which continues requirements laid out in the EU Habitats Directive (European Commission, 1992).

Developing regular accounts of marsh extents has previously been impeded by available technology. Traditional methods include the in-situ marking of extents using GPS systems, as well as the manual delineation of shorelines from aerial imagery. Carrying out these approaches at the regional to national scale required for coastal decision-making (Pontee, 2017) is extremely time and resource-intensive, which is of particular issue for the often underfunded Coastal Groups entrusted with developing SMPs (Pottier et al., 2005; Ballinger and Dodds, 2020).

Optical satellite remote sensing has the potential to provide the data required to understand historical changes in marsh extents and incorporate salt marshes into coastal decision-making. Optical satellites collect reflectance data across the visible and infrared spectrum which is discretised into spectral bands (e.g., green, or red). These bands can then be used to calculate spectral indices (SIs), which enhance contrast in the reflectance of different materials. In the case of salt marsh monitoring, vegetation indices (VIs) are commonly used such as the Normalized Difference Vegetation Index (NDVI), which measures plant photosynthetic activity. This approach, combined with machine learning, has been used to generate a variety of data in marshes such as vegetation cover (Kumar and Sinha, 2014; Laengner et al., 2019; Lopes et al., 2020), vegetation condition (Lopes et al., 2019, 2020), vegetation communities (Friess et al., 2012; van Beijma et al., 2014; Sun et al., 2018; Villoslada et al., 2020), aboveground biomass (Campbell and Wang, 2020) and carbon storage (Cao and Tzortziou, 2021; Ladd et al., 2021; Villoslada et al., 2022). Additionally, water indices have been used to map intertidal areas both in Australia (Sagar et al., 2017; Bishop-Taylor et al., 2019) and the UK (Fitton et al., 2021).

Satellite remote sensing is also an inherently scalable approach to monitoring, with global coverage, a return time of a few days and a historical record over several decades. This scalability has been further enhanced by the advent of the Google Earth Engine (GEE) (Gorelick et al., 2017). Previously, the storage and processing power required to analyse data over large areas has inhibited the use of satellite data (Schaeffer et al., 2013; Gorelick et al., 2017). GEE overcomes this issue by providing a multi-petabyte library of geospatial data including satellite products that can then be processed over the cloud. This has enabled large-scale analysis of coastal wetlands across the globe, including in Iran (Mafi-Gholami et al., 2019), Mexico (Celis-Hernandez et al., 2022), across Europe (Laengner et al., 2019) and even globally (Campbell et al., 2022; Murray et al., 2022). As this processing is carried out in the cloud, the GEE also reduces the resource and expertise requirements for decision-makers, thus making it more useable for management.

However, whilst there is substantial evidence of the value of satellite remote sensing for monitoring salt marshes and other coastal habitats, there has been little uptake of this technology in coastal management (Ouellette and Getinet, 2016). This limited use in management has been attributed to a lack of understanding amongst decision-makers, particularly regarding its value and low associated costs (Schaeffer et al., 2013). Consequently, it is essential that the value of this approach is communicated to decision-makers to ensure they have the best tools to inform coastal protection planning.

This study demonstrates the value of this technology in the Severn Estuary, UK. The Severn Estuary is a large, transboundary system with complex management strategies (Ballinger and Stojanovic, 2010), ultimately increasing the need for a sound information base for decision-making. Additionally, a large amount of salt marsh lines its edges, which provide considerable ecosystem services (Dargie, 1999; Armstrong et al., 2020), although there have been no recent formal reviews of their status.

To map marsh extents, a Random Forest (RF) algorithm was developed in the GEE using Landsat imagery, with training data derived from previous extent surveys carried out by national government agencies. This was undertaken across six areas containing some of the most significant areas of salt marsh across the Severn Estuary, with the accuracy of the derived extents assessed using validation testing. Marsh widths were also extracted to provide an indication of the coastal protection provided by marshes in the Severn Estuary as width of the vegetated area has been found to one of the most important predictors of the wave attenuation provided by the intertidal area (Willemsen et al., 2020). This study asked the overarching research question "can Landsat derived from GEE provide valuable insights into changes in salt marsh extents and widths in the Severn Estuary, which can be used for coastal protection?"

2. Study area

This study explored changes in salt marsh extents in the Severn Estuary, located in the south-west of the UK, with both English and Welsh banks (Fig. 1) and is one of the largest coastal plain estuaries in the UK. The area is protected for its importance, with the entire estuary designated as Special Area of Conservation (SAC), and the majority also designated as a Special Protection Area (SPA), Ramsar site and Site of Special Scientific Interest (SSSI). The estuary also contains three major cities: Cardiff, Newport, and Bristol, with a major port at Avonmouth.

The estuary experiences hyper tidal conditions, with a tidal range of

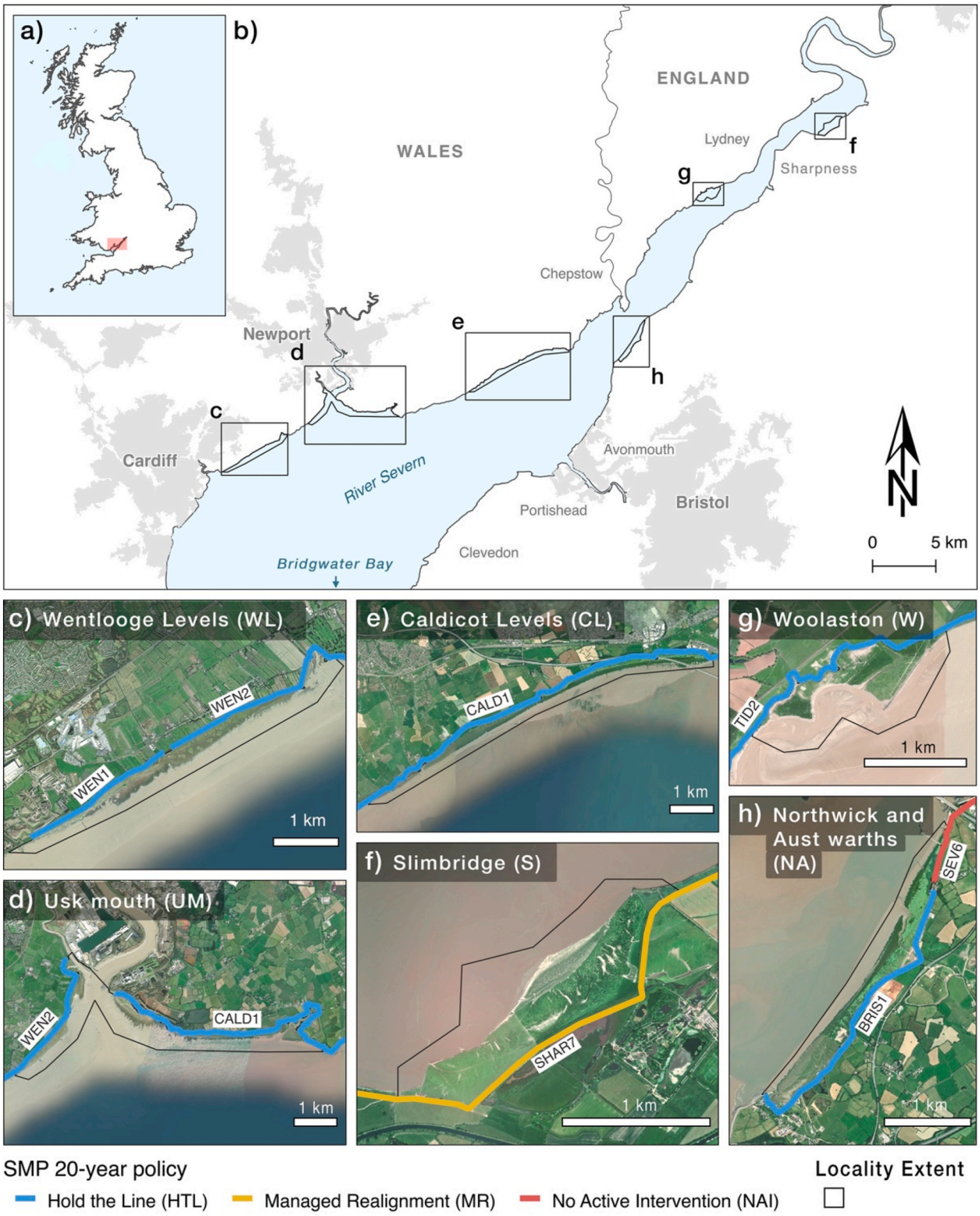

Fig. 1. The location of the Severn Estuary along with the localities focussed on in this study. Panel a shows the location of the Severn Estuary in the UK, b shows the estuary in greater detail, including the location of major towns and cities, the English/Welsh border and the localities. Panels c–h show close-up aerial photographs of the marshes in each locality, with the extent of the locality marked by the black line. The SMP PUs within each locality are also shown along with their 20-year policy. The white line in the bottom right of panels c–h marks 1 km. Aerial imagery in panels c–h was sourced from Esri.

14.8 m as a result of the coastal morphology (Allen and Duffy, 1998; Manning et al., 2010). The high tidal range results in a high-energy system, with average tidal velocities from 0.6 to 1.5 m s^{-1} (Manning et al., 2010). This high energy, combined with substantial fluvial inputs causes high turbidity in the estuary, with 1.3×10^7 and 9×10^6 tonnes of sediment suspended at spring and neap tides respectively (Collins, 1987; Allen, 1990a). This turbidity is greatest at two Estuarine Turbidity Maxima (ETM), one upstream of Sharpness and one in Bridgwater Bay

(Manning et al., 2010) (Fig. 1).

The marshes of the Severn Estuary are largely of the estuarine fringing type (Allen, 2000). These marshes are morphologically irregular as instead of the sinuous channels that are found across much of Europe, channels are straight as a result of the very high tidal range (Chatters, 2017). The most extensive study of vegetation in the area was carried out by Dargie (1999), which found 15 National Vegetation Classification (NVC) communities across low, mid and high marsh areas.

To explore changes in salt marsh extents in the estuary, we focussed on six areas that contain some of the most significant areas of salt marsh. This decision was made as many of the marshes are very narrow making them unsuitable for detection with Landsat's relatively coarse 30 m resolution (Laengner et al., 2019). We determined these areas using previous salt marsh surveys (NRW [unpublished], EA, 2020) and also published literature (e.g., Allen, 1990b; Haslett and Allen, 2014). The chosen areas were the Wentlooge Levels (WL), Usk mouth (UM) and Caldicot Levels (CL) on the Welsh side of the estuary, and Woolaston (W), Slimbridge (S) and Northwick and Aust warths (NA) on the English side of the estuary which are shown in Fig. 1.

HTL is the dominant policy across this area across the 20-year epoch as can be seen in Fig. 1, with most units maintaining the same policy over the 50- and 100-year epochs (SECG Atkins, 2017). The only exceptions are the SEV6 PU in NA, which maintains an NAI policy across the all epochs, W, in which the HTL policy changes to MR in the 100-year epoch, and S, which switches from MR to HTL for the 50- and 100-year epochs.

For analysis, the landward border of each of the salt marsh areas set to the high water mark which was determined from the Ordnance Survey Boundary-Line™ shapefile (Ordnance Survey, 2022). This data set is created by the Ordnance Survey and maps the approximate high-water mark across the United Kingdom. This data set was then manually adjusted where salt marsh areas were known to be inland of this line.

3. Methodology

A flow chart is provided in Fig. 2 demonstrating each of the steps used to generate the salt marsh extent and width data. Landsat images were taken from 1985 to 2020. This imagery was prepared for analysis by first adding spectral indices (SIs) and then by taking an annual mean from images across each year. Training and validation data were generated from previous salt marsh surveys carried out by national government agencies and used to label pixels from the annual mean of the same year as either 'salt marsh' or 'not salt marsh.' These labelled pixels were then split into training and validation sets by 80%:20%. Training data were then combined for all the survey dates to train a Random Forest (RF) model that was assessed for accuracy using the validation data from each survey. The trained model was then used to classify the annual means from 1985 to 2020 to generate the extents, with the widths calculated from the resultant extents.

3.1. Data

3.1.1. Landsat surface reflectance

Landsat-5 Thematic Mapper (TM), Landsat-7 Enhanced Thematic Mapper (ETM+) and Landsat-8 Operational Land Imager (OLI) Surface Reflectance (SR) data were collated for analysis. SR is a level-2 product, which has been atmospherically corrected to ensure continuity in the imagery. Landsat-5 covers the period from 01/01/1984 to 05/05–2012, Landsat-7 covers the period from 01/01/1999 to present, and Landsat-8 covers the period from 11/04/2013 to present, all with a spatial resolution of 30 m. Imagery was accessed through the Google Earth Engine (GEE) Python Application Programming Interface (API).

Images were initially filtered to those from 1st January 1985 to 31st December 2020 to ensure that each year had full coverage for reliable sampling. Images were then reduced to those with an image quality above 7 (0 being worst and 9 best; using the 'IMAGE QUALITY' field

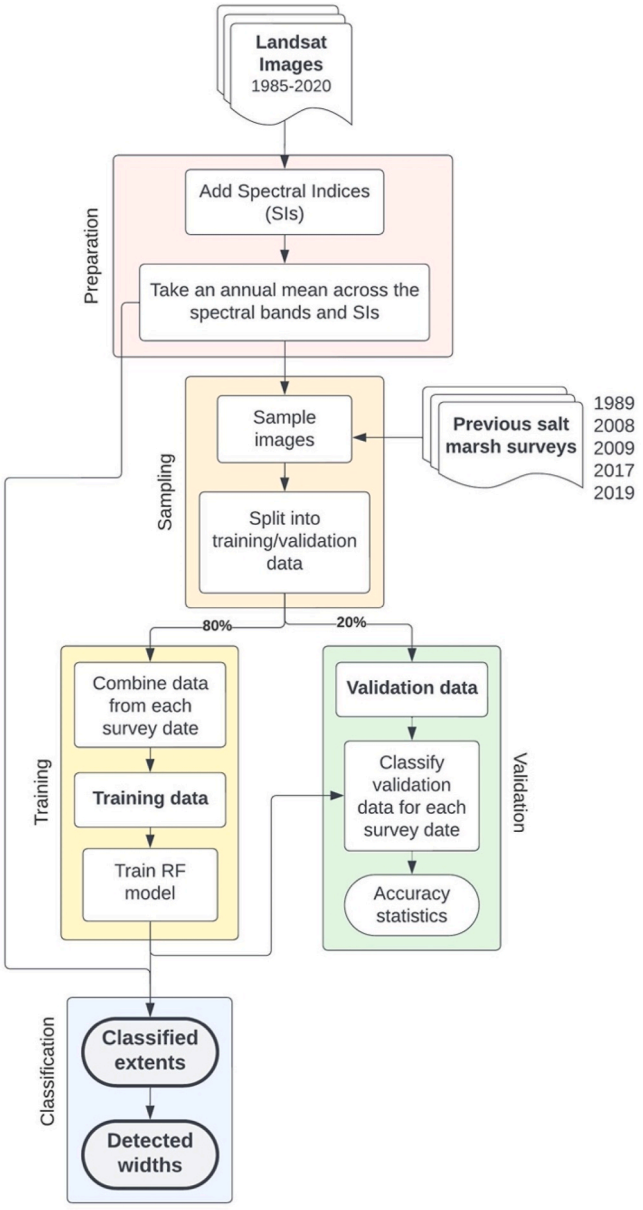

Fig. 2. Flow chart demonstrating the extent detection methods used in this study.

included in the metadata) and a cloud cover below 40% (using the 'CLOUD COVER' field in the metadata) to reduce the chance of anomalous pixels following the procedure outlined in Laengner et al. (2019). Images were also filtered to WRS Row/Path 24/203 to ensure each pixel was sampled at an equal frequency. Tidal stage was also considered to ensure the marshes were not flooded when the image was captured as flooding has been shown to influence spectral response (Beget and Di Bella, 2007). This was performed by comparing sensing times with data from the Avonmouth, Portbury and Newport tidal gauges accessed from the British Oceanographic Data Centre (BODC, 2023) as well as a visual assessment of images taken at high tides or where no tidal data were available. No images were found to have issues, with all the images taken at a tidal level below mean high water spring. This filtering produced a total of 178 images, the spread is shown in Fig. 3.

3.1.2. Spectral information

Three spectral indices (SIs) were included as inputs for the model and were chosen to enhance differences between salt marsh and non-salt

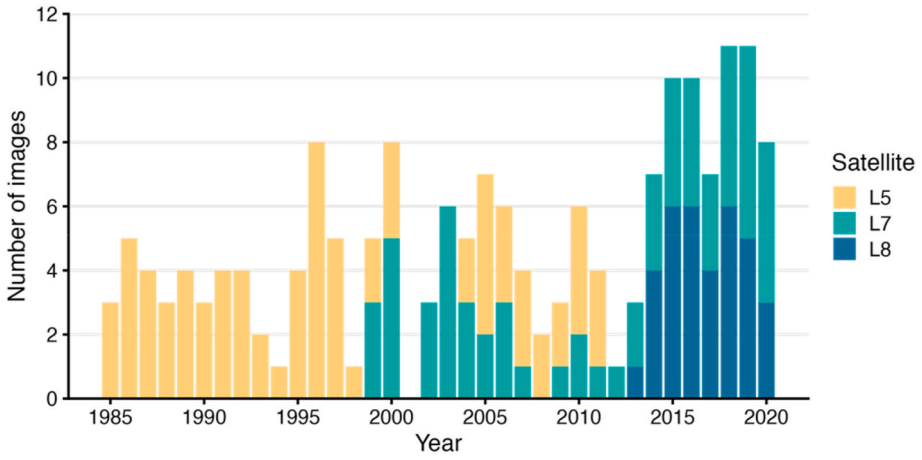

Fig. 3. Number of Landsat images collected in each year. L5 = Landsat-5, L7 = Landsat-7, and L8 = Landsat-8.

marsh areas. These SIs included two vegetation indices (VIs), the Normalized Difference Vegetation Index (NDVI) and the Modified Soil Adjusted Vegetation Index (mSAVI2) and the Normalized Difference Water Index (NDWI). These SIs were calculated from combinations of the green (G; TM/ETM+: 0.52–0.60 μm, OLI: 0.533–0.590 μm), red (R; TM/ETM+: 0.63–0.69 μm, OLI: 0.636–0.673 μm) and near infrared (NIR; TM/ETM+: 0.77–0.90 μm, OLI: 0.851–0.879 μm) bands.

NDVI was conceived by Rouse et al. (1974) is one of the most widely used VIs for differentiating vegetated and non-vegetated areas as it is based upon the high reflectance of NIR wavelengths and low reflectance of R wavelengths from chlorophyll.

$$\mathrm{NDVI} = \frac{\mathrm{NIR} - \mathrm{R}}{\mathrm{NIR} + \mathrm{R}}$$

mSAVI2 was also included as it was designed to perform better than NDVI in cases where there is high reflectance across bare ground or low vegetation cover (Qi et al., 1994), which may be the case across mudflats.

$$\mathrm{mSAVI2} = \frac{\left(2 \times \mathrm{NIR} + 1 - \sqrt{(2 \times \mathrm{NIR} + 1)^2 - 8 \times (\mathrm{NIR} - \mathrm{R})}\right)}{2}$$

NDWI is commonly used for detecting water in images and was included to ensure any flooded intertidal areas were removed. It takes advantage of the high reflectance of G wavelengths and low reflectance of NIR wavelengths in water (McFeeters, 1996).

$$\mathrm{NDWI} = \frac{\mathrm{G} - \mathrm{NIR}}{\mathrm{G} + \mathrm{NIR}}$$

3.1.3. Salt marsh extent surveys

Previous salt marsh extent surveys were included for both training and testing purposes. These surveys have been carried out by national government agencies in England and Wales, the Environment Agency (EA) and Natural Resources Wales (NRW) and are shown in Table 1.

Table 1
Previous surveys of salt marsh extents carried out in the Severn Estuary. NRW = Natural Resources Wales, EA = the Environment Agency (England).

Country	Date	Reference
Wales	1989	(NRW, unpublished)
	2008	(NRW, unpublished)
	2009	(NRW, unpublished)
	2017	(NRW, unpublished)
England	2008	EA (2020)
	2019	EA (2020)

3.2. Training and validation sampling

The previous extent surveys shown in Table 1 were used to create classified shapefiles across each of the salt marsh areas in which polygons were coded either as 0 which reflected 'not salt marsh' or 1 which reflected 'salt marsh' areas. The classified shapefiles were imported into the GEE where they were used to label the pixel values that fell within the classified polygons as 0 or 1.

Pixel values were sampled from an annual mean which was calculated per pixel across the SIs. The decision to use an annual mean, rather than individual images, aimed to a) to reduce the effect of missing data in individual images such as from the removal cloud pixels and from the broken scanning line corrector in Landsat-7, and b) as the exact date the extent surveys (Table 1) were carried out was not available. The average annual means and standard deviation per model, SI and class ('not salt marsh' and 'salt marsh') are shown in Table 2. The low values for the average standard deviation demonstrate there was relatively little temporal variation in pixel values, with the average annual standard deviation lower than the standard deviation in pixel values per model, SI and class in all cases. The standard deviation of each class is also lower than the difference in mean SI values between each class, further

Table 2
The average annual mean and average annual standard deviation (SD) of pixel values for the three models. The annual mean and standard deviation summarise temporal variation in pixel values within a year and are calculated as the mean value/standard deviation per pixel of all images in a year. These pixel values have been sampled using shapefiles from the previous surveys shown in Table 1, with the mean (± standard deviation) calculated from the images per model, SI and class.

Model	SI	Class	Average annual mean	Average annual SD
All	NDVI	Not SM	0.07 ± 0.15	0.07 ± 0.05
		SM	0.43 ± 0.17	0.11 ± 0.07
	NDWI	Not SM	−0.10 ± 0.15	0.08 ± 0.05
		SM	−0.41 ± 0.15	0.10 ± 0.07
	mSAVI2	Not SM	0.07 ± 1.76	0.16 ± 1.90
		SM	0.55 ± 2.31	0.14 ± 2.11
TM	NDVI	Not SM	0.07 ± 0.15	0.06 ± 0.05
		SM	0.43 ± 0.17	0.11 ± 0.08
	NDWI	Not SM	−0.10 ± 0.15	0.07 ± 0.05
		SM	−0.41 ± 0.15	0.10 ± 0.07
	mSAVI2	Not SM	0.07 ± 1.76	0.13 ± 1.90
		SM	0.54 ± 2.31	0.14 ± 2.11
OLI	NDVI	Not SM	0.11 ± 0.15	0.11 ± 0.07
		SM	0.51 ± 0.16	0.13 ± 0.07
	NDWI	Not SM	−0.14 ± 0.14	0.12 ± 0.07
		SM	−0.48 ± 0.13	0.12 ± 0.06
	mSAVI2	Not SM	0.13 ± 0.28	0.25 ± 0.25
		SM	0.64 ± 0.15	0.14 ± 0.08

demonstrating the temporal variability is negligible.

Samples were created for three models: a combined model containing all the satellites, henceforth referred to as 'All,' as well as separate models containing both Landsat-5 and Landsat-7, which is referred to as the 'TM' model, and Landsat-8, which is referred to as the 'OLI' model. This was carried out because the bands derived from the Landsat-8 OLI sensor are slightly different to the bands from Landsat-5/7's TM/ETM+ sensor (Roy et al., 2016) and thus this approach tested whether this affects their accuracy and thus whether separate models would be more appropriate.

The pixel values from the three annual mean SI maps were sampled from both classes ('salt marsh' and 'not salt marsh'). Each locality was sampled separately based upon the previous surveys which are shown in Table 1. This sample was then split 80% for the training data and 20% for the validation data. The training data from each year was then merged using the 'ee.FeatureCollection.merge' function to produce a single, combined training data set for each of the models. The same function was used to combine the validation data for each of the previous surveys to assess year-on-year accuracy. The validation data was also merged to produce a single, combined validation set to assess the model's overall performance.

3.3. Random Forest model

Salt marsh extents were detected from 1985 to 2020 using a Random Forests (RF) model trained inside GEE using the 'ee.Classifier.smileRandomForest' function. RF is a supervised nonparametric ensemble classifier that grows a specified number of decision trees from a subset of the supplied training data with replacement (bagging). Individual trees are grown by splitting nodes based upon the Gini impurity criterion, which measures how often a randomly chosen element would be improperly classified. At each node of a decision tree, the algorithm considers different splits based on different features and their values. For each split, it calculates the Gini impurity for the two child nodes and selects the split that minimizes the weighted sum of Gini impurities. In the 'ee.Classifier.smileRandomForest' function, this process is continued until each leaf node contains a minimum of one training sample, with each leaf specifying a vote for a class (e.g., 'salt marsh'/'not salt marsh'). New data (e.g., testing data) is then passed through the trees in the RF, with the majority vote across all the trees then used as the final classification.

RF is one of the most widely used algorithms for land cover classification using remote sensing data (Phan et al., 2020) and has been demonstrated to outperform other algorithms in coastal wetlands (Martinez Prentice et al., 2021). This improved performance has been suggested to be due to the effective handling of outliers and its efficient performance with high-dimensional datasets (Mahdianpari et al., 2017; Xia et al., 2017). RF is also popular as few parameters must be optimised, making its application more straight-forward than alternative algorithms (Sievers et al., 2021).

We decided on 100 trees based upon pre-tests, which aligns with the recommendations of previous land cover classification studies (Ghimire et al., 2012; Cánovas-García et al., 2017). All other hyperparameters were left as their default value. Once trained, this model was then applied across the annual mean aggregates for each year.

3.4. Accuracy assessment

The validation data produced in Section 3.2 was used to test the accuracy of the derived model. This was achieved by applying the model to the validation data, with the prediction then compared with the validation data using a confusion matrix. This confusion matrix was used to calculate several accuracy statistics which are shown in Table 3.

User's accuracy (U_{ac}) is the proportion of pixels classified as 'salt marsh' that have been correctly classified (viz. are present in the reference image) and thus provides a complementary quantification of overestimations (commission error; commission error = 1 - U_{ac}).

Table 3
Accuracy statistics used in this study and their equations. TP = true positive, TN = true negative, FP = false positive, FN = false negative. Apart from O_{ac} which applies to the whole model, statistics are calculated for each class. For the 'salt marsh' class, TP = 'salt marsh' in the predicted data and the validation data, TN = 'not salt marsh' in the predicted and validation data, FP = 'salt marsh' in the predicted data but 'not salt marsh' in the validation data, and FN = 'not salt marsh' in the predicted data but 'salt marsh' in the validation data.

Statistic	Equation
User's accuracy	$U_{ac} = \frac{TP}{TP + FN}$
Producer's accuracy	$P_{ac} = \frac{TP}{TP + FP}$
Overall accuracy	$O_{ac} = \frac{TP + TN}{TP + TN + FP + FN}$
Goodness of Fit	$GOF = U_{ac} \times P_{ac}$

Producer's accuracy (P_{ac}) is the proportion of 'salt marsh' pixels in the reference map that have been correctly classified in the satellite-derived map and thus provides a complementary quantification of 'salt marsh' underestimations (omission errors; omission error = 1 - P_{ac}).

Overall accuracy (O_{ac}) is the proportion of correctly classified 'salt marsh' and 'no salt marsh' pixels in relation to the total number of pixels in the image.

The Goodness-of-Fit (GOF) metric is the product of the user's and producer's accuracy and indicates the degree of spatial overlap between reference and satellite-derived maps (Hargrove et al., 2006). GOF can vary between 0 and 1, the closer to 1 the better the spatial agreement. Previous studies have shown GOF metric provides a more representative accuracy assessment than O_{ac} in cases where one class dominates (Lopes et al., 2020).

3.5. Extent and width assessment

Salt marsh extents in the six areas across the Severn estuary were detected from 1985 to 2020. This was performed using the trained RF classifier which produced classified maps for each year, in which pixels were classified as either 'salt marsh' or 'not salt marsh.' The areal extent of salt marsh in each of the areas was then calculated by counting the number of 'salt marsh' pixels in and multiplying the sum by the area of a Landsat pixel in hectares (0.003 ha). Trends in areal extent were assessed in each of the areas using linear regression. Comparisons were also made between the detected extents and the extents determined in the previous surveys using the root mean square error (RMSE).

Changes in the widths of salt marsh from 1985 to 2020 were also assessed in each of the localities to provide an indication of changes in their capacity for coastal protection. The width of the vegetated area has been suggested to be one of the most important indicators of the coastal protection provided by marshes (Willemsen et al., 2020). Widths were determined from the derived Landsat extents using transects. One kilometre long transects were generated in each locality perpendicular to the coastline at a 100 m spacing using the Boundary-Line™ shapefile (Ordnance Survey, 2022). This data set is created by the Ordnance Survey and maps the approximate high-water mark across the United Kingdom. This shapefile was cropped to the Severn Estuary and then simplified to ensure transects were perpendicular to the general shoreline morphology rather than local features. This simplification procedure was performed using the 'Simplify' tool in QGIS set to a tolerance of 100 m, with smaller tributaries, creeks and harbour features also manually removed.

To determine the width of the salt marsh, salt marsh polygon data were used to clip the transects using the 'Clip' tool, again in QGIS. With the reference data, both NRW and the EA provided the data in polygon form. To use the Landsat data, a binary raster was exported from GEE into QGIS in which 1 = salt marsh and 0 = no salt marsh. This raster was

then polygonised using the 'Polygonize (raster to vector)' tool from GDAL, with the resultant polygon then used to clip the transects and the length in metres calculated using the OSGB36 coordinate system.

Trends in marsh widths were assessed using linear regression. The detected widths were also assessed in comparison to the reference widths, again with linear regression in the form reference ~ predicted to ensure the slopes were representative (Piñeiro et al., 2008), as well as with the RMSE. Width changes were also compared with policy statements outlined in the most recent SMP (SMP2; SECG Atkins, 2017) to compare whether policies match physical changes.

4. Results

4.1. Accuracy assessment

Comparing the accuracy assessment using the aggregated validation data for the three models, all three displayed a relatively similar performance, with $O_{ac} = 0.91$ for the All and TM models and 0.92 for the OLI model. Looking at the validation data aggregated by year reveals more about the accuracy of each model as can be seen in Fig. 4. Here we can see that O_{ac} for both the All and TM models remains relatively similar. OLI also has a higher O_{ac} than the All model when looking at the 2017 validation. However, O_{ac} drops below the All model in 2019. Both the U_{ac} and P_{ac} for the 'salt marsh' class showed slightly greater variation. However, GOF demonstrates that the TM and All models maintain very similar spatial agreement over each year, with the OLI model displaying a higher GOF in 2017 but lower in 2019. Whilst accuracies in the three models were similar, it was decided the TM model was most effective due to marginally higher accuracies and sensor consistency. As a result, this is the only model discussed further.

Breaking down the validation per year also reveals there has been a general increase in accuracy over time. However, both U_{ac} and P_{ac} for the 'salt marsh' class remain relatively similar throughout the period very little impact on the total extents.

Looking at the localities across the estuary, some general trends are revealed. Overall, WL and UM displayed the lowest accuracies, with a GOF of 0.59 and 0.65 in 2009 and 1989 respectively. Comparatively S had the highest accuracy, with a GOF of 0.91 in 2019. W also showed a high accuracy, with a GOF of 0.88 in 2008.

The variable importance for the TM model is shown in Fig. 5. VIs were most important, with NDVI proving to be the most important variable, followed closely by mSAVI2. NDWI was the least important variable in the model.

4.2. Areal extent changes

Detected changes in the areal extent of the localities across the Severn Estuary found a significant ($p < 0.05$) increasing trend across three of the six (Fig. 6), namely CL, S and UM (Fig. 1). Increases were greatest in CL, where extents were found to have increased from 136.0 ha in 1985 to 141.0 ha in 2020, with a trend of +1.0 ha yr^{-1}. Comparatively, W was the only unit to show a decrease in extents, from 80.0 ha in 1985 to 47.3 ha in 2020. W also displayed the most consistent

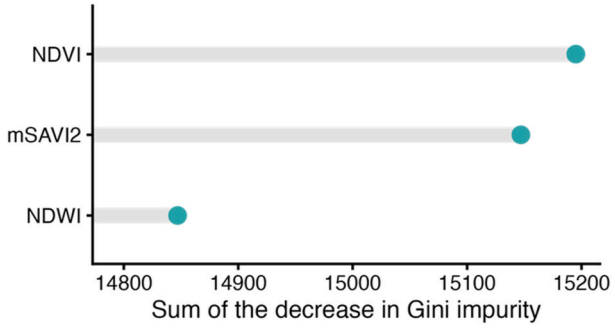

Fig. 5. Variable importance for the variables included in the TM model. Importance is shown as the sum of the decrease in Gini impurity over all trees in the model.

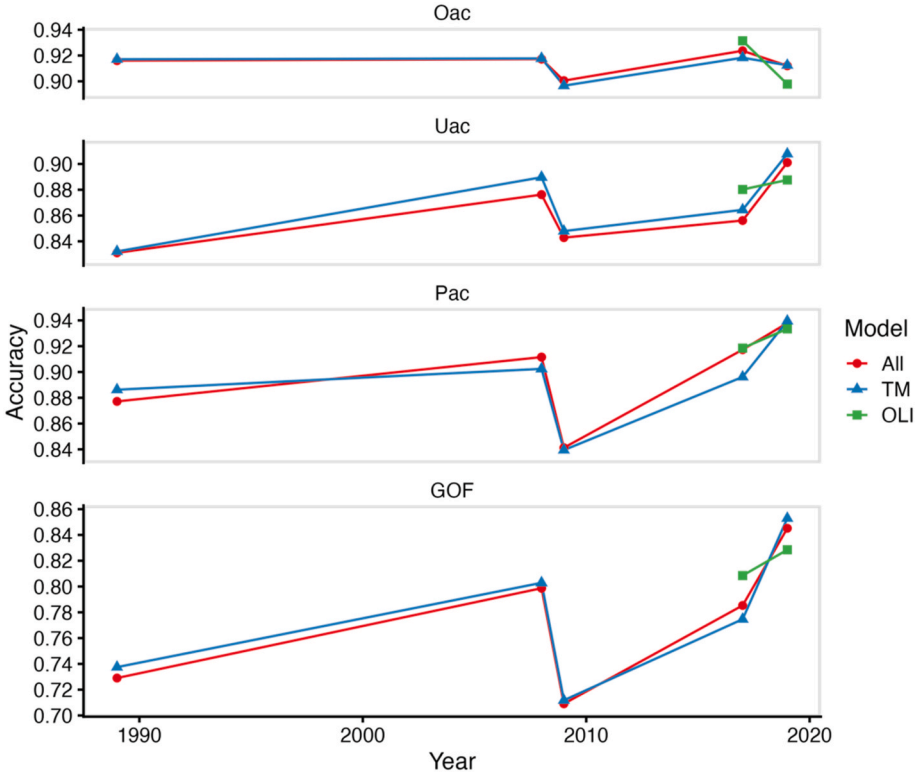

Fig. 4. Accuracy results for the three models. Each facet demonstrates a different accuracy statistic. U_{ac}, P_{ac} and GOF refer to the accuracy of the salt marsh class.

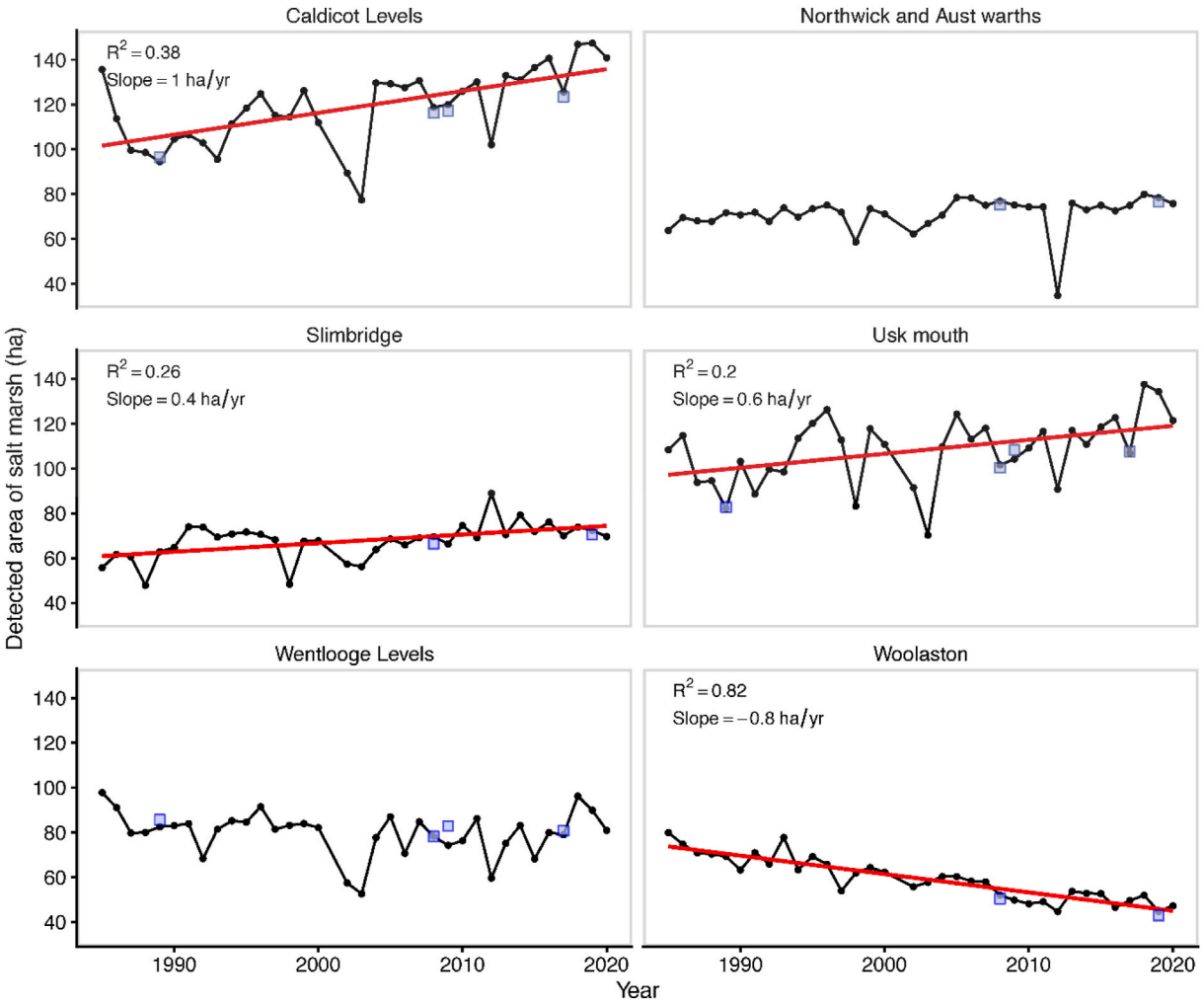

Fig. 6. Changes in the detected area of salt marsh in each locality across the Severn Estuary from 1985 to 2020 from the TM model. Trend lines are shown in red for localities which were found to have a significant ($p < 0.05$) trend using linear regression (viz. not NA or WL). Blue squares show the extents recorded in the previous extent surveys carried out by NRW/EA for comparison (more details in Table 1). (For interpretation of the references to colour in this figure legend, the reader is referred to the Web version of this article.)

trend, with the linear regression showing a decrease of 0.8 ha yr^{-1} and the change in year able to explain 82% of the variation in extents with a highly significant trend ($p < 0.001$). Both NA and WL did not show a significant trend ($p = 0.21$ and 0.29 respectively), with extents remaining largely the same although with some substantial interannual variations. Large interannual variations were also seen in the other areas, with many units showing a decrease in extent after 1999, with a subsequent increase between 2002 and 2004. Almost all the areas showed a sharp decrease in extent in 2012 with a subsequent increase in 2013, with NA showing the most pronounced change. The only exception was S, which demonstrated an increase in 2012 and subsequent decrease in 2013. Overall, interannual changes were least pronounced in W.

Comparing extents detected in this study to those in previous surveys shows a relatively good agreement, with the detected extents largely capturing the changes seen between these surveys (Fig. 6). The greatest disagreement can be seen in WL, with an RMSE between the detected extents and the previous surveys of 4.72 ha. Most of this error can be seen in 1985 and in 2009. The remaining units showed a much stronger agreement, with W showing the greatest agreement with an RMSE of 1.64 ha.

4.3. Width changes

Similar trends were seen in widths as in extents which can be seen in Fig. 7. CL, S and UM, as with their extents, showed significant ($p < 0.05$) increasing trends in mean width. This increase was greatest in S, which showed an increasing trend of 1.4 m yr^{-1} followed by CL at 1.2 m yr^{-1}. W also showed a significant ($p < 0.05$) decreasing trend of −3.7 m yr^{-1} with an R^2 of 0.84. WL and NA, as with extents, also showed no significant ($p < 0.05$) trend in widths. Similar inter-annual changes were seen in width as to extents, with a drop in mean width after 1999 and in 2012 seen in most units. However, inter-annual changes were less pronounced than with extents.

Overall, a strong agreement was found between detected widths and widths from previous surveys as can be seen in Fig. 8. When broken up into each locality and date of the survey (as the facets are in Figs. 8), 13 out of the18 showed the detected salt marsh widths explained over 90% of the variation in actual salt marsh widths. Of all the localities, detected extents explained most of the variation in W, with a mean R^2 of 0.99, while NA showed the lowest error, with a mean RMSE of 19 m. Comparatively, detected extents in CL explained the least of the variation, with a mean R^2 of 0.89, making it the only locality with a mean $R^2 < 0.9$, while WL showed the greatest error, with a mean RMSE of 27.5. Both R^2 and RMSE appeared to increase over time with a mean R^2 and RMSE of 0.91 23.3 m in 1989, and 0.97 and 20.3 m in 2019. There was,

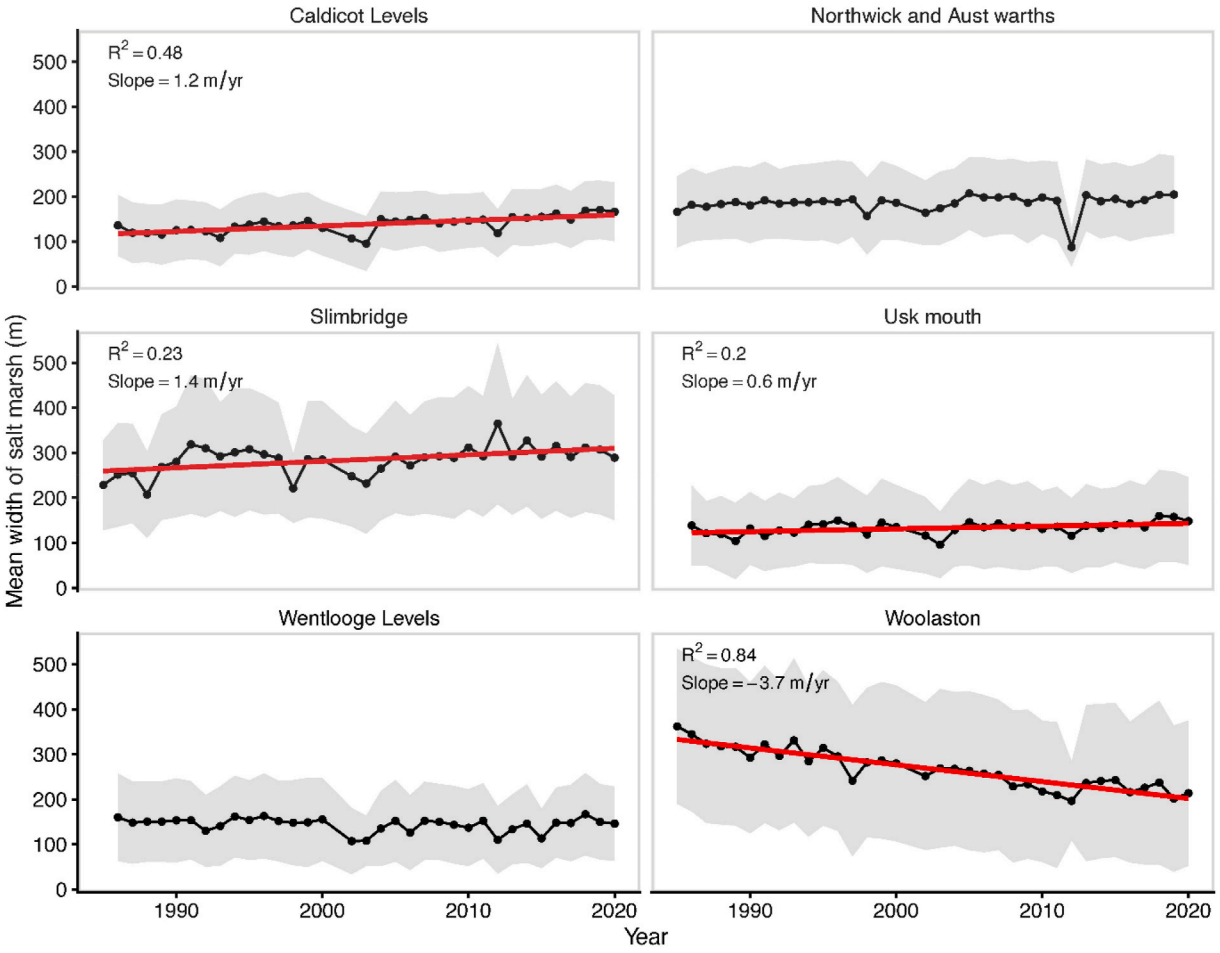

Fig. 7. Changes in detected salt marsh width across each locality from 1985 to 2020 from the TM model. The greyed area shows the standard deviation around the mean. Trend lines are shown in red for localities which were found to have a significant ($p < 0.05$) trend using linear regression (viz. not NA or WL). (For interpretation of the references to colour in this figure legend, the reader is referred to the Web version of this article.)

however, an exception in 2009 which showed the lowest agreement, with a mean R^2 and RMSE of 0.88 and 29.3 m respectively.

5. Discussion

5.1. Model accuracy

The accuracy assessment in this toolset shows that the RF model used in this study provides robust results using an easy-to-use series of methods that could be utilised to rapidly evaluate coastal wetland extent and change detection for coastal wetlands in the UK and beyond. This accuracy was demonstrated through confusion matrix validation testing, where an overall accuracy of 92% and GOF of 0.8 was found for the model, as well as through the comparisons between the detected widths and widths from previous surveys used as reference data, with detected widths able to explain 85%–99% of the variation in the reference widths. RF has been found to provide high classification accuracies in many other coastal wetland studies (e.g., Villoslada et al., 2020; Jia et al., 2021; Martinez Prentice et al., 2021; Rummell et al., 2022) and thus the findings of this study further support statements of its value in these settings.

Comparing the accuracy of the three models found that they each performed nearly equally well. The TM model showed a slightly higher accuracy than the All and OLI models which was likely due to the consistency of the TM and ETM+ sensors. However, the similar performance of the three models demonstrates that differences between the TM/ETM+ and OLI sensors had relatively little effect on the classifications, despite differences in the wavelengths of some bands (Roy et al., 2016). This suggests that differences in the spectral response between mudflats and salt marshes are greater than spectral differences between the two sensors. Thus, future studies aiming to differentiate these two classess may reasonably include both sensors.

The validation testing did reveal notable errors in some of the classifications. This error was greatest in the UM locality. Looking at the salt marsh present in the unit (Fig. 1), most of the marsh is relatively narrow, evident in the low detected widths (Fig. 7). UM demonstrated some of the narrowest widths of the localities, along with WL, which also showed a lower classification accuracy. Looking closer at the marshes in UM and WL reveals they also display a more complex marsh edge, with a ridge-runnel edge visible in UM in Fig. 1. Previous studies have found there is a greater error in classification at the marsh edge, attributed to the difficulty in classifying areas of marsh smaller than Landsat's 30 m resolution (Laengner et al., 2019; Lopes et al., 2020). This is the case for the marsh edge features in these areas and this study demonstrates that marsh edge morphology may affect classification accuracies. The converse of this effect can be seen in the higher classification accuracies of the S and W localities, which contain larger marsh platforms with simpler marsh edges as can be seen in Fig. 1.

5.2. Salt marsh extent changes

Significant increasing trends ($p < 0.05$) were found between 1985 and 2020 in three out of the six localities in the Severn estuary (CL, S, and WL). These increases go against suggsestions that there has been a

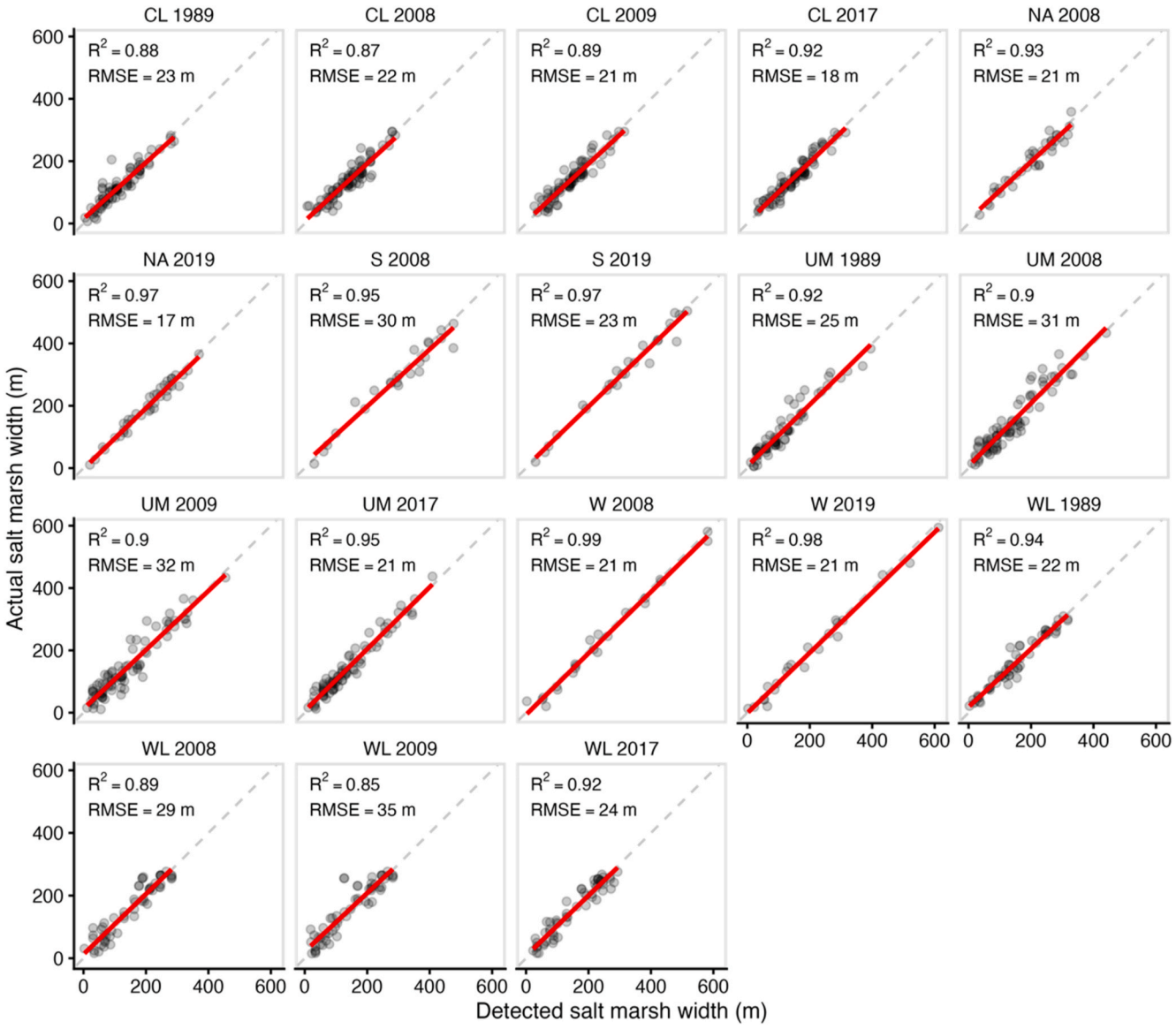

Fig. 8. Comparison between detected widths from the TM model and those from previous surveys facetted by each locality and the date of the survey. Each point represents the length of a transect. The solid, red line demonstrates a linear regression between the predicted and actual data. The dashed line represents an ideal 1:1 relationship. (For interpretation of the references to colour in this figure legend, the reader is referred to the Web version of this article.)

widespread decrease in marsh extents in recent decades (MEA, 2005; Deegan et al., 2012; European Commission, 1992), although recent studies have also observed increases in other estuaries (Ladd et al., 2019; Laengner et al., 2019; Murray et al., 2022). Conditions in the Severn Estuary favour expansion due to the estuary's hyper-tidal range. High tidal ranges increase suspended sediment concentrations (SSCs), which in turn facilitates marsh accretion and expansion (Reed, 1995; Kirwan and Guntenspergen, 2010; Ward et al., 2016a; Ward et al., 2016b; Schuerch et al., 2018; Ward and de Lacerda, 2021). High SSCs are known to be found in the Severn, with up to 10×10^6 tonnes of mud in suspension during spring tides and concentrations of 10–100 g l^{-1} in the turbidity maximum zones (Manning et al., 2010). As a result, the findings of this study may provide further evidence of this mechanism.

The high significance of the increasing trend in these localities suggests expansion will continue, at least into the near future. Changes in conditions could alter this trend. For example, rising sea levels over the 21st century may threaten marshes, even in highly resilient systems such as the Severn Estuary (Phillips and Crisp, 2010; Church et al., 2013; Horton et al., 2018). Mariotti and Fagherazzi (2010) showed that for any given sediment supply marshes can expand or erode depending on the rate of mean sea level rise, with high rates resulting in high currents, thus inducing erosion. Phillips and Crisp (2010) observed a reduction in tidal range over the period 1993–2007, which, if continued, could reduce its effect on marsh resilience. However, a recent modelling study by Mariotti (2020) suggested that erosion is rare in mesotidal (2–4 m) systems with high sediment supply even under high rates of RSLR (10 mm yr^{-1}), suggesting the hyper-tidal (14.8 m tidal range) Severn will remain resilient.

Despite increases at most localities, W saw a significant decreasing trend in both marsh extents and widths ($p < 0.05$). Edge erosion occurs in areas with low sediment budgets (Brooks et al., 2021), suggesting that sediment supply is lower in this area. As sediment dynamics in the Severn Estuary are highly complex and relatively poorly understood (Manning et al., 2010), it is difficult to determine whether this is the case in all three units. However, W is located south of an estuarine turbidity maxima at Sharpness (Manning et al., 2010), suggesting this may be drawing sediment away from this area. This is further supported by the significant increasing trend in both extents and widths at S ($p < 0.05$),

which is further upstream of this turbidity maxima.

5.3. Satellite remote sensing for coastal protection

As we have gained increased traction in the availability of remotely sensed data, whether from low resolution, long term and freely available global data such as MODIS or Landsat, to shorter term, higher resolution data sets such as the global SENTINEL or national LiDAR sources, to local drone derived data, researchers have been provided with a range of new tools to undertake coastal monitoring assessments (Mafi-Gholami et al., 2019; Veettil et al., 2020; Villoslada et al., 2022). This, combined with the Google Earth Engine, which integrates a range of freely available data in one place, together with a series of toolsets to select atmospherically corrected data with cloud cover removal and cover assessment algorithms, has significantly improved the accessibility of these datasets as well as improved their usability. These changes have made remote sensing a valuable tool for decision-makers.

Wave attenuation provided by a salt marsh has been found to be a function of its width (Willemsen et al., 2020). The width increases observed in the majority of localities in this study therefore suggest a widespread improvement in the natural coastal protection provided by the marshes in these areas. This information, coupled with the significance of the increasing trends, suggests existing sea defences across much of the estuary may be sustainable with future sea level rise given observed expansion in response to current rates. As a result, this suggests the HTL policy across most of the PUs in these areas will be sustainable.

Marsh expansion was, however, not observed across all the areas. A strong significant ($p < 0.05$) decreasing trend was found at W. The current SMP states a HTL policy over the next 20-year and 50-year epochs in the TID2 PU, which covers the W area (SECG Atkins, 2017). This decreasing trend suggests that this HTL policy may not be sustainable, particularly considering the strength and high significance of the trend which suggests it will continue. The policy for the TID2 unit switches to MR for the 100-year epoch. This change in policy fits the observed changes in extents. However, given the current rate of decreases in width, marshes in the area could disappear in the next 52 years suggesting a change in policy may be required sooner. Additionally, if current losses are due to a lack of sediment supply to the area then it may be expected that limited marsh development may occur under the MR policy (Day et al., 2021). As a result, the findings of this study suggest a reappraisal of the policies in this PU should be made.

Direct quantification of the wave attenuation provided by salt marshes is valuable for coastal decision-making as this data could be translated into the design of existing sea defences including their sustainability (Bouma et al., 2014). Rates of attenuation have been given in the literature; for example, Möller and Spencer (2002) suggested wave heights were dissipated by 0.5% per metre across two marshes on the UK's east coast. Additionally, these figures could aid the translation of attenuation rates into monetary value, which would also aid decision-making, both for cost-benefit-analyses and stakeholder engagement (zu Ermgassen et al., 2021). However, the relationship between marsh width and wave attenuation has been suggested to be non-linear, making the use of simplistic percentage per metre statistics misleading (Möller et al., 2001; Koch et al., 2009). Consequently, further development is required before such figures can be operational.

A major benefit of using the automated approach developed in this study for shoreline management is the ability to produce a time-series that can be used to explore significant trends within the data. Traditional methods (e.g., manual delineation from aerial imagery) are prohibitively resource-intensive to carry out frequently across areas above a local scale thus preventing the development of regional time-series datasets. Comparatively, the open-access nature of Landsat (as well as other satellite missions such as Sentinel), combined with the free-to-use GEE, enables high temporal resolution monitoring at up to a global scale with very little resource requirements (Gorelick et al., 2017; Murray et al., 2022), a factor that is particularly important in the traditionally underfunded world of coastal management (Schaeffer et al., 2013; Ballinger and Dodds, 2020).

The trends observed in this study from the long time-series provide valuable insights into long-term ecosystem dynamics to inform future policy and engineering. This is an essential aspect of coastal planning (Pontee, 2017). However, this has been identified as the main knowledge gap preventing the inclusion of natural systems in this process (Bouma et al., 2014). The method applied in this study therefore provides a positive improvement in this area and may, with further development, facilitate a greater awareness of the role of salt marshes in protection management and for other applications such as blue carbon accounting. Additionally, the ability to attach significance to these trends associated with the time-series data ensures decision-makers can be confident in the quality of the data, which is essential for robust adaptation planning (Nicholls et al., 2013; Brown, 2022).

The validation testing used in this study provides evidence that satellite remote sensing may effectively derive salt marsh extents and widths to inform coastal decision-making, particularly at the regional scale. There were, however, inaccuracies in some areas, particularly in delineating marsh features close to the Landsat's 30 m resolution. As a result, this method may not be practical for monitoring narrower marshes such as those in the Severn Estuary outside of the six localities, which were focussed on in this study.

One potential way to reduce the errors in the data is to use Sentinel-2 instead of Landsat which has an improved resolution of 10 m. This improvement in resolution has been found to have a marked improvement on the accuracy of delineated marsh extents and shorelines (Campbell and Wang, 2020; Blount et al., 2022). However, Sentinel-2 was first launched in 2015, meaning it is not possible to create the almost 40-year time-series possible with Landsat. As a result, both should be considered to have their own independent advantages (Veettil et al., 2020). Going forwards, Sentinel-2 will likely provide a more accurate understanding of the coastal protection provided by marshes, particularly at the local scale, with already almost a decade's worth of data to provide context. However, for the long-term understanding of changes in ecosystem dynamics and at a larger scale, Landsat remains the better choice.

In this study, the near 1:1 slope observed between the predicted widths and actual widths demonstrates that the errors have not affected the overall prediction of widths. The understanding of the effect of the detection errors on the estimates of marsh width provided by the validation data used in this study is essential for decision-making (Schaeffer et al., 2013; Ouellette and Getinet, 2016). As a result, it is vital that if a satellite-based approach to monitoring the coastline is used, validation data is also collected to provide an accuracy assessment. At first glance, this could be considered to negate the value of using satellite monitoring. However, the higher temporal resolution of satellite data means that gaps between the validation data can be filled, providing the benefits of a long time-series. For example, the Saltmarsh Change data set created by the Environment Agency (2020) is carried out every ten years. The method used in this study therefore provides nine records of marsh extents between each Saltmarsh Change survey. As this data is integrated into testing and training the RF model, this approach can lead to a continual improvement in the accuracy of detected extents as further reference data is included.

An important factor in coastal decision-making is taking a large-scale approach (Pontee, 2017). As a result, it is vital that the data used to aid this decision-making supports wider spatial planning to enable its use as a key decision-support tool (Potts et al., 2013). As satellites have a global coverage, they fit well into this requirement, with studies demonstrating that marshes can be monitored at international scales (Laengner et al., 2019; Murray et al., 2022). The Severn Estuary represents a highly challenging environment to analyse due to its hyper-tidal range and narrow, fringing marshes, suggesting the methods used in this study could be transferable to other large marsh areas and thus scalable across larger areas.

6. Conclusion

This study demonstrated that, with a relatively simple automated classification method applied to Landsat imagery, valuable insights could be derived about the coastal protection provided by salt marshes surrounding the Severn Estuary. Overall, marsh extents and widths were found to have increased across most of the areas focussed on in the estuary between 1985 and 2019 with a significant ($p < 0.05$) positive trend, suggesting an increase in their natural protective capacity. This increase in marsh area is likely due to observed high suspended sediment concentrations in the estuary, creating positive sediment budgets in marshes that are likely to facilitate expansion. Although increases were widespread, a significant ($p < 0.05$) decreasing trend was observed in W. The current SMP document gives W a HTL policy which may not be sustainable considering these findings. In turn, this also demonstrates how the derived data can be used for policy evaluation.

The ability to identify the significance of trends in extents is a major benefit of satellite remote sensing as it can aid projections into the future. Other methods that have been assess changes in marsh extents would be prohibitively resource-intensive to carry out at the temporal frequency and scale achieved in this study. The most substantial drawback in the use of satellites is their vulnerability to classification errors. However, the validation testing found these errors were low in the model used in this study and the comparison between detected widths and those determined in previous surveys found a strong agreement. Additionally, as this is a fast-evolving field, continued work will likely reduce these errors as methods and sensors improve. As a result, satellite-derived products, such as used in this study, should be considered a valuable asset to shoreline management planning.

CRediT authorship contribution statement

Joseph Agate: Writing – review & editing, Writing – original draft, Visualization, Software, Project administration, Methodology, Formal analysis, Conceptualization. **Rhoda Ballinger:** Writing – review & editing, Supervision, Methodology. **Raymond D. Ward:** Writing – review & editing, Writing – original draft.

Declaration of competing interest

The authors state they have no conflicts of interest in this submission.

Data availability

The Google Earth Engine code has been included in the supplementary material.

Acknowledgements

The authors would like to thank Natural Resources Wales for providing shapefiles of salt marsh on the Welsh side of the Severn Estuary. The authors also thank Dr Niels Andela for the valuable advice he provided during the development of the methodology. The authors would also like to thank the reviewers of this paper whose valuable comments helped improve its quality.

Appendix A. Supplementary data

Supplementary data to this article can be found online at https://doi.org/10.1016/j.ecss.2024.108639.

References

Allen, J.R.L., 1990a. The Severn Estuary in southwest Britain: its retreat under marine transgression, and fine-sediment regime. Sediment. Geol. 66, 13–28. https://doi.org/10.1016/0037-0738(90)90003-C.

Allen, J.R.L., 1990b. Salt-marsh growth and stratification: a numerical model with special reference to the Severn Estuary, southwest Britain. Mar. Geol. 95, 77–96. https://doi.org/10.1016/0025-3227(90)90042-I.

Allen, J.R.L., 2000. Morphodynamics of holocene salt marshes: a review sketch from the atlantic and southern north sea coasts of Europe. Quat. Sci. Rev. 19, 1155–1231. https://doi.org/10.1016/S0277-3791(99)00034-7.

Allen, J.R.L., Duffy, M.J., 1998. Medium-term sedimentation on high intertidal mudflats and salt marshes in the Severn Estuary, SW Britain: the role of wind and tide. Mar. Geol. 150, 1–27. https://doi.org/10.1016/S0025-3227(98)00051-6.

Armstrong, S., Hull, S., Pearson, Z., Kay, S., Wilson, R., 2020. Estimating the Carbon Sink Potential of the Welsh Marine Environment (NRW Evidence Report No. 428). ABPmer, Cardiff.

Ballinger, R.C., Dodds, W., 2020. Shoreline management plans in England and Wales: a scientific and transparent process? Mar. Pol. 111 https://doi.org/10.1016/j.marpol.2017.03.009.

Ballinger, R., Stojanovic, T., 2010. Policy development and the estuary environment: a Severn Estuary case study. Mar. Pollut. Bull. 61, 132–145. https://doi.org/10.1016/j.marpolbul.2009.12.020.

Beaumont, N., Townsend, M., Mangi, S., Austen, M.C., 2006. Marine Biodiversity – an Economic Valuation.

Beget, M.E., Di Bella, C.M., 2007. Flooding: the effect of water depth on the spectral response of grass canopies. J. Hydrol. 335, 285–294. https://doi.org/10.1016/j.jhydrol.2006.11.018.

Bertram, C., Quaas, M., Reusch, T.B.H., Vafeidis, A.T., Wolff, C., Rickels, W., 2021. The blue carbon wealth of nations. Nat. Clim. Change 11, 704–709. https://doi.org/10.1038/s41558-021-01089-4.

Bishop-Taylor, R., Sagar, S., Lymburner, L., Beaman, R.J., 2019. Between the tides: modelling the elevation of Australia's exposed intertidal zone at continental scale. Estuar. Coast Shelf Sci. 223, 115–128. https://doi.org/10.1016/j.ecss.2019.03.006.

Blount, T.R., Carrasco, A.R., Cristina, S., Silvestri, S., 2022. Exploring open-source multispectral satellite remote sensing as a tool to map long-term evolution of salt marsh shorelines. Estuarine. Coastal and Shelf Science 266, 107664. https://doi.org/10.1016/j.ecss.2021.107664.

BODC, 2023. UK Tide Gauge Network [WWW Document]. URL https://www.bodc.ac.uk/data/hosted_data_systems/sea_level/uk_tide_gauge_network/processed/. . (Accessed 12 August 2023).

Bouma, T.J., van Belzen, J., Balke, T., Zhu, Z., Airoldi, L., Blight, A.J., Davies, A.J., Galvan, C., Hawkins, S.J., Hoggart, S.P.G., Lara, J.L., Losada, I.J., Maza, M., Ondiviela, B., Skov, M.W., Strain, E.M., Thompson, R.C., Yang, S., Zanuttigh, B., Zhang, L., Herman, P.M.J., 2014. Identifying knowledge gaps hampering application of intertidal habitats in coastal protection: opportunities & steps to take. Coast. Eng. 87, 147–157. https://doi.org/10.1016/j.coastaleng.2013.11.014.

Brooks, H., Möller, I., Carr, S., Chirol, C., Christie, E., Evans, B., Spencer, K.L., Spencer, T., Royse, K., 2021. Resistance of salt marsh substrates to near-instantaneous hydrodynamic forcing. Earth Surf. Process. Landforms 46, 67–88. https://doi.org/10.1002/esp.4912.

Brown, I., 2022. Do habitat compensation schemes to offset losses from sea level rise and coastal squeeze represent a robust climate change adaptation response? Ocean Coast Manag. 219, 106072 https://doi.org/10.1016/j.ocecoaman.2022.106072.

Callaghan, D.P., Bouma, T.J., Klaassen, P., van der Wal, D., Stive, M.J.F., Herman, P.M.J., 2010. Hydrodynamic forcing on salt-marsh development: distinguishing the relative importance of waves and tidal flows. Estuar. Coast Shelf Sci. 89, 73–88. https://doi.org/10.1016/j.ecss.2010.05.013.

Campbell, A.D., Wang, Y., 2020. Salt marsh monitoring along the mid-Atlantic coast by Google Earth Engine enabled time series. PLoS One 15, e0229605. https://doi.org/10.1371/journal.pone.0229605.

Campbell, A.D., Fatoyinbo, L., Goldberg, L., Lagomasino, D., 2022. Global hotspots of salt marsh change and carbon emissions. Nature 612, 701–706. https://doi.org/10.1038/s41586-022-05355-z.

Cánovas-García, F., Alonso-Sarría, F., Gomariz-Castillo, F., Oñate-Valdivieso, F., 2017. Modification of the random forest algorithm to avoid statistical dependence problems when classifying remote sensing imagery. Comput. Geosci. 103, 1–11. https://doi.org/10.1016/j.cageo.2017.02.012.

Cao, F., Tzortziou, M., 2021. Capturing dissolved organic carbon dynamics with Landsat-8 and Sentinel-2 in tidally influenced wetland–estuarine systems. Sci. Total Environ. 777, 145910 https://doi.org/10.1016/j.scitotenv.2021.145910.

Celis-Hernandez, O., Villoslada-Peciña, M., Ward, R.D., Bergamo, T.F., Perez-Ceballos, R., Girón-García, M.P., 2022. Impacts of environmental pollution on mangrove phenology: combining remotely sensed data and generalized additive models. Sci. Total Environ. 810, 152309 https://doi.org/10.1016/j.scitotenv.2021.152309.

Chatters, C., 2017. Saltmarsh. Bloomsbury Natural History, London, New York.

Church, J.A., Clark, P.U., Cazenave, A., Gregory, J.M., Jevrejeva, S., Levermann, A., Merrifield, M.A., G.A. Milne, R.S., Nerem, P.D.N., Payne, A.J., Pfeffer, W.T., Stammer, D., Unnikrishnan, A.S., 2013. Sea level change. In: Stocker, T.F., Qin, D., Plattner, G.-K., Tignor, M., Allen, S.K., Boschung, J., Nauels, A., Xia, Y., Bex, V., Midgley, P.M. (Eds.), Climate Change 2013: the Physical Science Basis. Contribution of Working Group I to the Fifth Assessment Report of the Intergovernmental Panel on Climate Change. Cambridge University Press, Cambridge, United Kingdom and New York, NY, USA.

Collins, M., 1987. Sediment transport in the Bristol channel: a review. PGA (Proc. Geol. Assoc.) 98, 367–383. https://doi.org/10.1016/S0016-7878(87)80076-7.

Committee on Climate Chaange, 2018. Managing the Coast in a Changing Climate.

Dargie, T., 1999. NVC Survey of Saltmarsh Habitat in the Severn Estuary 1998 (CCW Contract Science Report No. NO. 341). Countryside Council for Wales. English Nature.

Day, J., Burdick, D.M., Ibáñez, C., Mitsch, W.J., Elsey-Quirk, T., Rivaes, S., 2021. Restoration of tidal marshes. In: FitzGerald, D.M., Hughes, Z.J. (Eds.), Salt Marshes: Function, Dynamics, and Stresses. Cambridge University Press, Cambridge, pp. 443–475. https://doi.org/10.1017/9781316888933.020.

Deegan, L.A., Johnson, D.S., Warren, R.S., Peterson, B.J., Fleeger, J.W., Fagherazzi, S., Wollheim, W.M., 2012. Coastal eutrophication as a driver of salt marsh loss. Nature 490, 388–392. https://doi.org/10.1038/nature11533.

Defra, 2020. Flood and Coastal Erosion Risk Management: Policy Statement.

EA, 2020. Saltmarsh change [WWW Document]. Saltmarsh Change. URL https://data.gov.uk/dataset/2d5d8f23-3582-491b-aae4-c987ffabb910/saltmarsh-change. . (Accessed 1 October 2021).

Ermgassen, P.S.E., Baker, R., Beck, M.W., Dodds, K., zu Ermgassen, S.O.S.E., Mallick, D., Taylor, M.D., Turner, R.E., 2021. Ecosystem services: delivering decision-making for salt marshes. Estuar. Coast 44, 1691–1698. https://doi.org/10.1007/s12237-021-00952-z.

European Commission, 1992. The Habitats Directive.

Fitton, J.M., Rennie, A.F., Hansom, J.D., Muir, F.M.E., 2021. Remotely sensed mapping of the intertidal zone: a Sentinel-2 and Google Earth Engine methodology. Remote Sens. Appl.: Society and Environment 22, 100499. https://doi.org/10.1016/j.rsase.2021.100499.

French, P.W., 2004. The changing nature of, and approaches to, UK coastal management at the start of the twenty-first century. Geogr. J. 170, 116–125.

Friess, D.A., Spencer, T., Smith, G.M., Möller, I., Brooks, S.M., Thomson, A.G., 2012. Remote sensing of geomorphological and ecological change in response to saltmarsh managed realignment, the Wash, UK. Int. J. Appl. Earth Obs. Geoinf. 18, 57–68. https://doi.org/10.1016/j.jag.2012.01.016.

Ghimire, B., Rogan, J., Galiano, V.R., Panday, P., Neeti, N., 2012. An evaluation of bagging, boosting, and random Forests for land-cover classification in cape cod, Massachusetts, USA. GIScience Remote Sens. 49, 623–643. https://doi.org/10.2747/1548-1603.49.5.623.

Gorelick, N., Hancher, M., Dixon, M., Ilyushchenko, S., Thau, D., Moore, R., 2017. Google Earth engine: planetary-scale geospatial analysis for everyone. Rem. Sens. Environ. https://doi.org/10.1016/j.rse.2017.06.031.

Hargrove, W.W., Hoffman, F.M., Hessburg, P.F., 2006. Mapcurves: a quantitative method for comparing categorical maps. J. Geogr. Syst. 8, 187. https://doi.org/10.1007/s10109-006-0025-x.

Haslett, S.K., Allen, J.R.L., 2014. Salt-marsh evolution at Northwick and Aust warths, Severn Estuary, UK: a case of constrained autocyclicity. atgeol 50, 1–17. https://doi.org/10.4138/atlgeol.2014.001.

HM Government, 2017. The Conservation of Habitats and Species Regulations.

Horton, B.P., Shennan, I., Bradley, S.L., Cahill, N., Kirwan, M., Kopp, R.E., Shaw, T.A., 2018. Predicting marsh vulnerability to sea-level rise using Holocene relative sea-level data. Nat. Commun. 9, 2687. https://doi.org/10.1038/s41467-018-05080-0.

Jia, M., Wang, Z., Mao, D., Ren, C., Wang, C., Wang, Y., 2021. Rapid, robust, and automated mapping of tidal flats in China using time series Sentinel-2 images and Google Earth Engine. Rem. Sens. Environ. 255, 112285 https://doi.org/10.1016/j.rse.2021.112285.

Jones, L., Angus, S., Cooper, A., Doody, P., Everard, M., Garbutt, A., Gilchrist, P., Hansom, J.D., Nicholls, R., Pye, K., Ravenscroft, N., Rees, S., Rhind, P., Whitehouse, A., 2011. Chapter 11: coastal margins. In: UK National Ecosystem Technical Report, pp. 411–459. Cambridge.

King, S.E., Lester, J.N., 1995. The value of salt marsh as a sea defence. Mar. Pollut. Bull. 30, 180–189. https://doi.org/10.1016/0025-326X(94)00173-7.

Kirwan, M.L., Guntenspergen, G.R., 2010. Influence of tidal range on the stability of coastal marshland. J. Geophys. Res.: Earth Surf. 115 https://doi.org/10.1029/2009JF001400.

Koch, E.W., Barbier, E.B., Silliman, B.R., Reed, D.J., Perillo, G.M., Hacker, S.D., Granek, E.F., Primavera, J.H., Muthiga, N., Polasky, S., Halpern, B.S., Kennedy, C.J., Kappel, C.V., Wolanski, E., 2009. Non-linearity in ecosystem services: temporal and spatial variability in coastal protection. Front. Ecol. Environ. 7, 29–37. https://doi.org/10.1890/080126.

Kumar, L., Sinha, P., 2014. Mapping salt-marsh land-cover vegetation using high-spatial and hyperspectral satellite data to assist wetland inventory. GIScience Remote Sens. 51, 483–497. https://doi.org/10.1080/15481603.2014.947838.

Ladd, C.J.T., Duggan-Edwards, M.F., Bouma, T.J., Pagès, J.F., Skov, M.W., 2019. Change in Saltmarsh Extent for Six Regions across Great Britain, pp. 1846–2016.

Ladd, C.J.T., Skov, M.W., Austin, W.E.N., Smeaton, C., 2021. Best Practice for Generating Spatial Predictions of Soil Organic Carbon Stock in Salt Marshes ([Preprint]).

Laengner, M.L., Siteur, K., van der Wal, D., 2019. Trends in the seaward extent of saltmarshes across Europe from long-term satellite data. Rem. Sens. 11, 1653. https://doi.org/10.3390/rs11141653.

Lopes, C.L., Mendes, R., Caçador, I., Dias, J.M., 2019. Evaluation of long-term estuarine vegetation changes through Landsat imagery. Sci. Total Environ. 653, 512–522. https://doi.org/10.1016/j.scitotenv.2018.10.381.

Lopes, C.L., Mendes, R., Caçador, I., Dias, J.M., 2020. Assessing salt marsh extent and condition changes with 35 years of Landsat imagery: tagus Estuary case study. Rem. Sens. Environ. 247, 111939 https://doi.org/10.1016/j.rse.2020.111939.

Luisetti, T., Jackson, E.L., Turner, R.K., 2013. Valuing the European 'coastal blue carbon' storage benefit. Mar. Pollut. Bull. 71, 101–106. https://doi.org/10.1016/j.marpolbul.2013.03.029.

Macreadie, P.I., Anton, A., Raven, J.A., Beaumont, N., Connolly, R.M., Friess, D.A., Kelleway, J.J., Kennedy, H., Kuwae, T., Lavery, P.S., Lovelock, C.E., Smale, D.A., Apostolaki, E.T., Atwood, T.B., Baldock, J., Bianchi, T.S., Chmura, G.L., Eyre, B.D., Fourqurean, J.W., Hall-Spencer, J.M., Huxham, M., Hendriks, I.E., Krause-Jensen, D., Laffoley, D., Luisetti, T., Marbà, N., Masque, P., McGlathery, K.J., Megonigal, J.P., Murdiyarso, D., Russell, B.D., Santos, R., Serrano, O., Silliman, B.R., Watanabe, K., Duarte, C.M., 2019. The future of Blue Carbon science. Nat. Commun. 10, 3998. https://doi.org/10.1038/s41467-019-11693-w.

Mafi-Gholami, D., Zenner, E.K., Jaafari, A., Ward, R.D., 2019. Modeling multi-decadal mangrove leaf area index in response to drought along the semi-arid southern coasts of Iran. Sci. Total Environ. 656, 1326–1336. https://doi.org/10.1016/j.scitotenv.2018.11.462.

Mahdianpari, M., Salehi, B., Mohammadimanesh, F., Motagh, M., 2017. Random forest wetland classification using ALOS-2 L-band, RADARSAT-2 C-band, and TerraSAR-X imagery. ISPRS J. Photogrammetry Remote Sens. 130, 13–31. https://doi.org/10.1016/j.isprsjprs.2017.05.010.

Manning, A.J., Langston, W.J., Jonas, P.J.C., 2010. A review of sediment dynamics in the Severn Estuary: influence of flocculation. Mar. Pollut. Bull. 61, 37–51. https://doi.org/10.1016/j.marpolbul.2009.12.012.

Mariotti, G., 2020. Beyond marsh drowning: the many faces of marsh loss (and gain). Adv. Water Resour. 144, 103710 https://doi.org/10.1016/j.advwatres.2020.103710.

Mariotti, G., Fagherazzi, S., 2010. A numerical model for the coupled long-term evolution of salt marshes and tidal flats. J. Geophys. Res.: Earth Surf. 115 https://doi.org/10.1029/2009JF001326.

Martinez Prentice, R., Villoslada Peciña, M., Ward, R.D., Bergamo, T.F., Joyce, C.B., Sepp, K., 2021. Machine learning classification and accuracy assessment from high-resolution images of coastal wetlands. Rem. Sens. 13, 3669. https://doi.org/10.3390/rs13183669.

McFeeters, S.K., 1996. The use of the Normalized Difference Water Index (NDWI) in the delineation of open water features. Int. J. Rem. Sens. 17, 1425–1432. https://doi.org/10.1080/01431169608948714.

MEA, 2005. Ecosystems and Human Well-Being: A Framework for Asessment. Washington, DC. URL. https://www.millenniumassessment.org/en/Framework.html.

Möller, I., 2006. Quantifying saltmarsh vegetation and its effect on wave height dissipation: results from a UK East coast saltmarsh. Estuarine, Coastal and Shelf Science. Salt Marsh Geomorphology: Physical and ecological effects on landform 69, 337–351. https://doi.org/10.1016/j.ecss.2006.05.003.

Möller, I., Spencer, T., 2002. Wave dissipation over macro-tidal saltmarshes: effects of marsh edge typology and vegetation change. J. Coast Res. 506–521. https://doi.org/10.2112/1551-5036-36.sp1.506.

Möller, I., Spencer, T., French, J.R., Leggett, D.J., Dixon, M., 1999. Wave transformation over salt marshes: a field and numerical modelling study from north norfolk, England. Estuarine. Coastal and Shelf Science 49, 411–426. https://doi.org/10.1006/ecss.1999.0509.

Möller, I., Spencer, T., French, J.R., Leggett, D.J., Dixon, M., 2001. The Sea-defence value of salt marshes: field evidence from north norfolk. Water Environ. J. 15, 109–116. https://doi.org/10.1111/j.1747-6593.2001.tb00315.x.

Möller, I., Kudella, M., Rupprecht, F., Spencer, T., Paul, M., van Wesenbeeck, B.K., Wolters, G., Jensen, K., Bouma, T.J., Miranda-Lange, M., Schimmels, S., 2014. Wave attenuation over coastal salt marshes under storm surge conditions. Nat. Geosci. 7, 727–731. https://doi.org/10.1038/ngeo2251.

Murray, N.J., Worthington, T.A., Bunting, P., Duce, S., Hagger, V., Lovelock, C.E., Lucas, R., Saunders, M.I., Sheaves, M., Spalding, M., Waltham, N.J., Lyons, M.B., 2022. High-resolution mapping of losses and gains of Earth's tidal wetlands. Science 376, 744–749. https://doi.org/10.1126/science.abm9583.

Nerem, R.S., Beckley, B.D., Fasullo, J.T., Hamlington, B.D., Masters, D., Mitchum, G.T., 2018. Climate-change–driven accelerated sea-level rise detected in the altimeter era. Proc. Natl. Acad. Sci. USA 115, 2022–2025. https://doi.org/10.1073/pnas.1717312115.

Nicholls, R.J., Townend, I.H., Bradbury, A.P., Ramsbottom, D., Day, S.A., 2013. Planning for long-term coastal change: experiences from England and Wales. Ocean Engineering, Sea Level Rise and Impacts on Engineering Practice 71, 3–16. https://doi.org/10.1016/j.oceaneng.2013.01.025.

Noujas, V., Thomas, K.V., 2018. Shoreline management plan for a medium energy coast along west coast of India. J. Coast Conserv. 22, 695–707. https://doi.org/10.1007/s11852-018-0602-4.

Ordnance Survey, 2022. Boundary-Line™, ordnance survey data hub. URL https://osdatahub.os.uk/downloads/open/BoundaryLine. . (Accessed 17 March 2023).

Ouellette, W., Getinet, W., 2016. Remote sensing for marine spatial planning and integrated coastal areas management: achievements, challenges, opportunities and future prospects. Remote Sens. Appl.: Society and Environment 4, 138–157. https://doi.org/10.1016/j.rsase.2016.07.003.

Phan, T.N., Kuch, V., Lehnert, L.W., 2020. Land cover classification using Google Earth engine and random forest classifier—the role of image composition. Rem. Sens. 12, 2411. https://doi.org/10.3390/rs12152411.

Phillips, M.R., Crisp, S., 2010. Sea level trends and NAO influences: the Bristol channel/severn estuary. Global Planet. Change 73, 211–218. https://doi.org/10.1016/j.gloplacha.2010.06.005.

Pickering, M.D., Horsburgh, K.J., Blundell, J.R., Hirschi, J.J.-M., Nicholls, R.J., Verlaan, M., Wells, N.C., 2017. The impact of future sea-level rise on the global tides. Continent. Shelf Res. 142, 50–68. https://doi.org/10.1016/j.csr.2017.02.004.

Piñeiro, G., Perelman, S., Guerschman, J., Paruelo, J., 2008. How to evaluate models: observed vs. Predicted or predicted vs. Observed? Ecol. Model. 216, 316–322. https://doi.org/10.1016/j.ecolmodel.2008.05.006.

Pontee, N., 2017. Coastal engineering and management. In: Green, D.R., Payne, J.L. (Eds.), Marine and Coastal Resource Management: Principles and Practice. Routledge, Oxford & New York, pp. 79–100.

Pottier, N., Penning-Rowsell, E., Tunstall, S., Hubert, G., 2005. Land use and flood protection: contrasting approaches and outcomes in France and in England and Wales. Appl. Geogr. 25, 1–27. https://doi.org/10.1016/j.apgeog.2004.11.003.

Potts, J.S., Carter, D., Taussik, J., 2013. Shoreline management: the way ahead. In: Managing Britain's Marine and Coastal Environment. Routledge, pp. 248–280.
Qi, J., Chehbouni, A., Huete, A.R., Kerr, Y.H., Sorooshian, S., 1994. A modified soil adjusted vegetation index. Rem. Sens. Environ. 48, 119–126. https://doi.org/10.1016/0034-4257(94)90134-1.
Reed, D.J., 1995. The response of coastal marshes to sea-level rise: survival or submergence? Earth Surf. Process. Landforms 20, 39–48. https://doi.org/10.1002/esp.3290200105.
Reguero, B.G., Losada, I.J., Méndez, F.J., 2019. A recent increase in global wave power as a consequence of oceanic warming. Nat. Commun. 10 https://doi.org/10.1038/s41467-018-08066-0.
Rouse, J.W., Haas, R.H., Schell, J.A., Deering, D.W., 1974. Monitoring Vegetation Systems in the Great Plains with ERTS.
Roy, D.P., Kovalskyy, V., Zhang, H.K., Vermote, E.F., Yan, L., Kumar, S.S., Egorov, A., 2016. Characterization of Landsat-7 to Landsat-8 reflective wavelength and normalized difference vegetation index continuity. Rem. Sens. Environ. 185, 57–70.
Rummell, A.J., Leon, J.X., Borland, H.P., Elliott, B.B., Gilby, B.L., Henderson, C.J., Olds, A.D., 2022. Watching the saltmarsh grow: a high-resolution remote sensing approach to quantify the effects of wetland restoration. Rem. Sens. 14, 4559. https://doi.org/10.3390/rs14184559.
Sagar, S., Roberts, D., Bala, B., Lymburner, L., 2017. Extracting the intertidal extent and topography of the Australian coastline from a 28year time series of Landsat observations. Rem. Sens. Environ. 195, 153–169. https://doi.org/10.1016/j.rse.2017.04.009.
Salman, A., Lombardo Doody, P., 2004. Living with coastal erosion in Europe. In: Sediment and Space for Sustainability, Eurosion Project Reports.
Schaeffer, B.A., Schaeffer, K.G., Keith, D., Lunetta, R.S., Conmy, R., Gould, R.W., 2013. Barriers to adopting satellite remote sensing for water quality management. Int. J. Rem. Sens. 34, 7534–7544. https://doi.org/10.1080/01431161.2013.823524.
Schuerch, M., Spencer, T., Temmerman, S., Kirwan, M.L., Wolff, C., Lincke, D., McOwen, C.J., Pickering, M.D., Reef, R., Vafeidis, A.T., Hinkel, J., Nicholls, R.J., Brown, S., 2018. Future response of global coastal wetlands to sea-level rise. Nature 561, 231–234. https://doi.org/10.1038/s41586-018-0476-5.
SECG, Atkins, 2017. Part B - policy statements. In: Severn Estuary Shoreline Management Plan Review.
Sievers, M., Brown, C.J., Buelow, C.A., Pearson, R.M., Turschwell, M.P., Fernanda Adame, M., Griffiths, L., Holgate, B., Rayner, T.S., Tulloch, V.J.D., Roy Chowdhury, M., zu Ermgassen, P.S.E., Yip Lee, S., Lillebø, A.I., Mackey, B., Maxwell, P.S., Rajkaran, A., Sousa, A.I., Connolly, R.M., 2021. Global typologies of coastal wetland status to inform conservation and management. Ecol. Indicat. 131, 108141 https://doi.org/10.1016/j.ecolind.2021.108141.
Sun, C., Fagherazzi, S., Liu, Y., 2018. Classification mapping of salt marsh vegetation by flexible monthly NDVI time-series using Landsat imagery. Estuar. Coast Shelf Sci. 213, 61–80. https://doi.org/10.1016/j.ecss.2018.08.007.
Temmerman, S., Meire, P., Bouma, T.J., Herman, P.M.J., Ysebaert, T., De Vriend, H.J., 2013. Ecosystem-based coastal defence in the face of global change. Nature 504, 79–83. https://doi.org/10.1038/nature12859.
UNEP, 2016. Options for Ecosystem-Based Adaptation (EBA) in Coastal Environments: A Guide for Environmental Managers and Planners. UNEP, Nairobi.
van Beijma, S., Comber, A., Lamb, A., 2014. Random forest classification of salt marsh vegetation habitats using quad-polarimetric airborne SAR, elevation and optical RS data. Rem. Sens. Environ. 149, 118–129. https://doi.org/10.1016/j.rse.2014.04.010.
Veettil, B.K., Ward, R.D., Lima, M.D.A.C., Stankovic, M., Hoai, P.N., Quang, N.X., 2020. Opportunities for seagrass research derived from remote sensing: a review of current methods. Ecol. Indicat. 117, 106560 https://doi.org/10.1016/j.ecolind.2020.106560.
Villoslada, M., Bergamo, T.F., Ward, R.D., Burnside, N.G., Joyce, C.B., Bunce, R.G.H., Sepp, K., 2020. Fine scale plant community assessment in coastal meadows using UAV based multispectral data. Ecol. Indicat. 111, 105979 https://doi.org/10.1016/j.ecolind.2019.105979.
Villoslada, M., Sipelgas, L., Bergamo, T.F., Ward, R.D., Reintam, E., Astover, A., Kumpula, T., Sepp, K., 2022. Multi-source remote sensing data reveals complex topsoil organic carbon dynamics in coastal wetlands. Ecol. Indicat. 143, 109329 https://doi.org/10.1016/j.ecolind.2022.109329.
Ward, R.D., de Lacerda, L.D., 2021. Chapter 10 - responses of mangrove ecosystems to sea level change. In: Sidik, F., Friess, D.A. (Eds.), Dynamic Sedimentary Environments of Mangrove Coasts. Elsevier, pp. 235–253. https://doi.org/10.1016/B978-0-12-816437-2.00002-1.
Ward, R.D., Burnside, N.G., Joyce, C.B., Sepp, K., Teasdale, P.A., 2016a. Improved modelling of the impacts of sea level rise on coastal wetland plant communities. Hydrobiologia 774, 203–216. https://doi.org/10.1007/s10750-015-2374-2.
Ward, Raymond D., Friess, D.A., Day, R.H., MacKenzie, R.A., 2016b. Impacts of climate change on mangrove ecosystems: a region by region overview. Ecosys. Health Sustain. 2, e01211 https://doi.org/10.1002/ehs2.1211.
Willemsen, P.W.J.M., Borsje, B.W., Vuik, V., Bouma, T.J., Hulscher, S.J.M.H., 2020. Field-based decadal wave attenuating capacity of combined tidal flats and salt marshes. Coast. Eng. 156, 103628 https://doi.org/10.1016/j.coastaleng.2019.103628.
Xia, J., Falco, N., Benediktsson, J.A., Du, P., Chanussot, J., 2017. Hyperspectral image classification with rotation random forest via KPCA. IEEE J. Sel. Top. Appl. Earth Obs. Rem. Sens. 10, 1601–1609. https://doi.org/10.1109/JSTARS.2016.2636877zu.